| Rivista Italiana di Paleontologia e Stratigrafia | volume 111 | no. 2 | 3 pls. | pp. 233-245 | July 2005 |
|---|---|---|---|---|---|

# MAGNETOSTRATIGRAPHY AND BIOSTRATIGRAPHY OF THE LATE TRIASSIC GURI ZI SECTION, ALBANIA: CONSTRAINT ON THE AGE OF THE CARNIAN-NORIAN BOUNDARY

GIOVANNI MUTTONI [1], SELAM MEÇO [2] & MAURIZIO GAETANI [1]

*Received: November 15, 2003; accepted: May 12, 2005*

*Key words*: Carnian-Norian boundary, Late Triassic, magnetostratigraphy, biostratigraphy, conodonts, Albania.

*Abstract*. We present the magnetostratigraphy and conodont biostratigraphy across the Carnian-Norian boundary from a 70 m-thick limestone section located at Guri Zi in northern Albania. A total of 14 magnetozones were observed. The Carnian-Norian boundary is placed in a thin stratigraphic interval between the last occurrence of *Paragondolella nodosa* and the first occurrence of *Epigondolella abneptis.* Data from Guri Zi are in substantial agreement with already published data from Silicka Brezova in Slovakia and Pizzo Mondello in Sicily, which complessively indicate that the conodont Carnian-Norian boundary, when magnetostratigraphically traced onto the Newark astrochronological polarity time scale (APTS), has an age of ~228-227 Ma.

*Riassunto*. In questo articolo vengono presentati i risultati di uno studio di magnetostratigrafia e biostratigrafia a conodonti condotto su una sezione di 70 m di spessore comprendente il limite Carnico-Norico e affiorante presso l'abitato di Guri Zi in Albania settentrionale. Sono state riconosciute 14 magnetozone. Il limite Carnico-Norico è stato posizionato in un sottile intervallo stratigrafico tra l'ultimo rinvenimento (last occurrence) di *Paragondolella nodosa* e il primo rinvenimento (first occurrence) di *Epigondolella abneptis.* I dati della sezione di Guri Zi sono in sostanziale accordo con dati di recente pubblicazione provenienti dalle sezioni di Silicka Brezova in Slovacchia e Pizzo Mondello in Sicilia. Questi dati indicano complessivamente che il limite Carnico-Norico basato sui conodonti, correlato magnetostratigraficamente alla scala temporale astro-magnetocronologica del bacino del Newark, ha età di ~228-227 Ma.

## Introduction

This paper presents the magnetostratigraphy and conodont biostratigraphy of a Carnian-Norian (Late Triassic) boundary section located at Guri Zi in northern Albania. This study adds to previous studies on the Tethyan conodont biostratigraphy and magnetostratigraphy across the Carnian-Norian boundary from Pizzo Mondello in Sicily (Muttoni et al. 2001a; Krystyn et al. 2002; Muttoni et al. 2004), Silicka Brezova in Slovakia (Channell et al. 2003), and Kavaalani in Turkey (Gallet et al. 2000). At Kavaalani, however, the Carnian-Norian boundary falls in correspondence of a hiathus. Aim of this work is to contribute to constrain magnetostratigraphically the position of the Carnian-Norian conodont boundary on the Newark continental astrochronological polarity time scale (APTS; Kent & Olsen 1999) for construction of a biostratigraphically calibrated time scale for the Late Triassic.

## Geology

During the Triassic-Jurassic, the Guri Zi and sorrounding regions were part of the eastern passive continental margin of Adria – the African promontory (Muttoni et al. 1996a) – and its transition to the adjoining Tethys Ocean. The Krasta-Cukali Zone, which comprises the Guri Zi section (Fig. 1), is interpreted as a rim basin on thinned continental crust located between the Mirdita rift shoulders-oceanic basin and the Adria passive continental margin of the Ionian Zone (Meço and Aliay 2000; Robertson et al. 1991; Godroli 1992; Kellici et al. 1994).

During Alpine deformation in the Mesozoic-Cenozoic, the Krasta Zone was tectonically overridden along its eastern flank by Mirdita Zone units consisting

1 Dipartimento di Scienze della Terra, Università di Milano, Via Mangiagalli 34, I-20133 Milan, Italy.
2 Fakulteti Gjeologji Miniera, Universiteti Politeknik, Tirana, Albania.

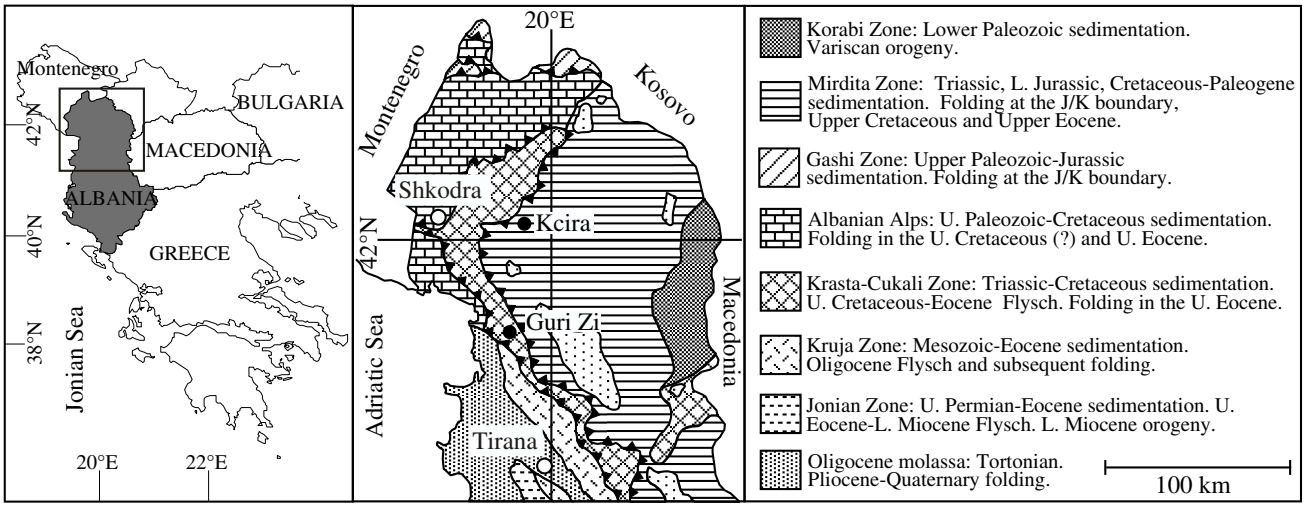


Fig. 1 - Simplified geologic map of Albania. The locations of the Guri Zi and Kçira sections are indicated.

of slabs of mainly Upper Triassic deep-sea sediments and Jurassic ophiolites (Shallo 1992; 1994). Krasta Zone units overrode to the west Mesozoic shallow-water carbonates of the Kruja and Ionian zones, which make transition further to the west to relatively undeformed carbonate successions pertaining to the Adria foreland.

The upper Carnian-middle Norian Guri Zi section is located 14 km southeast of the town of Shkodra, approximately 1 km to the east of the village of Guri Zi in northern Albania (42.05°N, 19.02°E; Fig. 1). The section is 70 m-thick (Fig. 2) and starts at the base with a few meters of Ladinian radiolarites followed by about 60 meters of Cherty Limestone beds. These consist of thinly bedded calcilutites with pelagic bivalves and chert nodules associated with more massive and sometimes slumped calcarenites and calcilutites. Towards the section top, Cherty Limestone beds are brecciated and form clasts enclosed in red matrix of unknown age. This brecciated interval is unconformably overlain by Maastrichtian (Upper Cretaceous) grey-green marls with Globotruncanids, which are in turn overlain by terrigenous deposits of the Paleogene Krasta Flysch.

## Biostratigraphy

We performed additional conodont sampling at Guri Zi after Meço (1999). Samples for conodont biostratigraphy were collected with an average sampling resolution of 2 m. A total of 36 samples, about 2-3 kilograms each, were obtained for dissolution in acetic acid.

Triassic stage boundaries are historically established using ammonoids. These have not been found at Guri Zi, whose age is therefore based on conodont biostratigraphy as a proxy for the ammonoid zonation. According to Krystyn et al. (2002), the ammonoid Carnian-Norian boundary is approximated by conodonts using the first occurrences (FOs) of *Metapolygnathus communisti* A, *Metapolygnathus communisti* B, or *Norigondolella navicula*. In addition, the last occurrences (LOs) of *Metapolygnathus polygnathiformis* and *Metapolygnathus nodosus* immediately predate the boundary, whereas the FO of *Epigondolella abneptis* A immediately postdates the boundary (Krystyn et al. 2002). Channell et al. (2003) reached similar conclusions regarding the FOs of *Norigondolella navicula* and *Epigondolella abneptis* (undifferentiated form), as well as the LOs of *Metapolygnathus polygnathiformis* and *Metapolygnathus nodosus.* These authors indicate in the FO of *Epigondolella primitia* an additional useful conodont event that immediately predates the Carnian-Norian boundary.

At Guri Zi, the following succession of biostratigraphic events defines complessively the Carnian-Norian boundary interval (Fig. 2):

(i) the LO of *Paragondolella polygnathiformis* (=*Metapolygnathus polygnathiformis*) juvenile (Figs. 1-3 in Plate 1);

(ii) the LO of *Metapolygnathus nodosus* (Figs. 11-14 in Plate 2);

(iii) the occurrence of *Epigondolella primitia* (Figs. 1, 2, 4 in Plate 3);

(iv) the FO of *Epigondolella abneptis* (Figs. 3, 6, 8 in Plate 3).

In particular, we locate the Carnian-Norian boundary in a thin stratigraphic interval around meter level 50 between the LO of *Metapolygnathus nodosus* and the FO of *Epigondolella abneptis*.

In the upper part of the section, around meter level 68, the occurrence of *Epigondolella multidentata* is recorded (Fig. 2). This conodont is regarded as middle Norian in age (Channell et al. 2003). We assume, therefore, the existence of a major hiathus at this level, which marks at a gross scale the base of the uppermost interval of brecciated limestones.

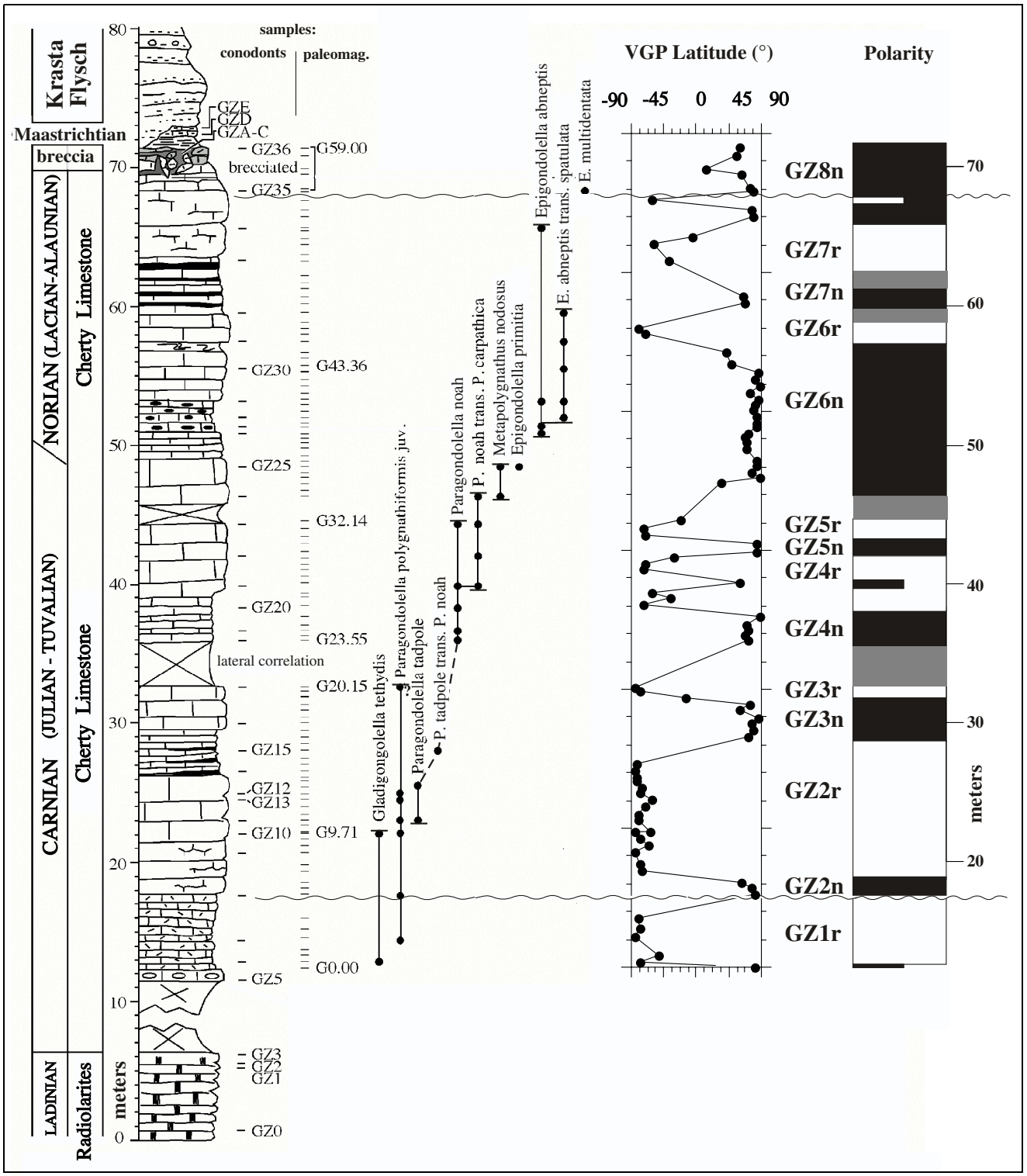


Fig. 2 - The Carnian-Norian boundary Guri Zi section. To the left of figure are the lithology column and the stratigraphic position of samples for paleomagnetism and biostratigraphy; the age determination is based on conodont biostratigraphy. To the right of figure is a plot of VGP latitudes as function of stratigraphic depth with polarity interpretation. Magnetic polarity zones, defined by at least two stratigraphically superposed samples, are shown by filled (open) bars for normal (reverse) polarity. Polarity zones defined by one sample are shown by half bars.

## Paleomagnetism

Samples from Guri Zi were drilled and oriented in the field at an average resolution of 50 cm giving 110 standard specimens (11 cc) for analysis. The extremely weak magnetization of Guri Zi limestones required the use of a high sensitivity magnetometer with DC SQUID technology, located in a magnetically shielded room at the paleomagnetic laboratory of ETH Zürich.

PLATE 1

Fig. 1 - *Paragondolella polygnathiformis* (Budurov & Stefanov), juvenile form; lateral view; 90x; sample GZ7; age: Carnian.
Fig. 2 - *Paragondolella polygnathiformis* (Budurov & Stefanov), juvenile form; lateral-upper view; 100x; sample GZ8; age: Carnian.
Fig. 3 - *Paragondolella polygnathiformis* (Budurov & Stefanov), juvenile form; lateral view; 100x; sample GZ10; age: Carnian.
Fig. 4 - *Paragondolella polygnathiformis* (Budurov & Stefanov); lateral view; 100x; sample GZ12; age: Carnian.
Fig. 5 - *Paragondolella tadpole* (Hayashi); lateral view; 90x; sample GZ11; age: Carnian.
Fig. 6 - *Paragondolella tadpole* (Hayashi); lateral view; 90x; sample GZ13; age: Carnian.
Fig. 7 - *Paragondolella tadpole* (Hayashi); upper view; 90x; sample GZ13; age: Carnian.
Fig. 8 - *Paragondolella tadpole* (Hayashi) - *Paragondolella noah* (Hayashi) transitional form; lateral view; 90x; sample GZ15; age: Carnian.
Fig. 9 - *Paragondolella tadpole* (Hayashi) - *Paragondolella noah* (Hayashi) transitional form; lateral view; 90x; sample GZ15; age: Carnian.
Fig. 10 - *Paragondolella tadpole* (Hayashi) - *Paragondolella noah* (Hayashi) transitional form; lateral view; 100x; sample GZ15; age: Carnian.
Fig. 11 - *Paragondolella tadpole* (Hayashi) - *Paragondolella noah* (Hayashi) transitional form; lateral view; 100x; sample GZ15; age: Carnian.
Fig. 12 - *Paragondolella noah* (Hayashi) - *Paragondolella carpathica* (Mock) transitional form; lateral view; 100x; sample GZ21; age: Carnian.
Fig. 13 - *Paragondolella noah* (Hayashi) - *Paragondolella carpathica* (Mock) transitional form; lateral view; 100x; sample GZ22; age: Carnian.
Fig. 14 - *Paragondolella noah* (Hayashi) - *Paragondolella carpathica* (Mock) transitional form; upper-lateral view; 100x; sample GZ22bis (same level as GZ22); age: Carnian.
Fig. 15 - *Paragondolella noah* (Hayashi) - *Paragondolella carpathica* (Mock) transitional form; lateral-upper view; 100x; sample GZ24; age: Carnian.
Fig. 16 - *Paragondolella noah* (Hayashi) - *Paragondolella carpathica* (Mock) transitional form; upper view; 100x; sample GZ22; age: Carnian.
Fig. 17 - *Paragondolella noah* (Hayashi) - *Paragondolella carpathica* (Mock) transitional form; lateral view; 100x; sample GZ22bis (same level as GZ22); age: Carnian.
Fig. 18 - *Paragondolella noah* (Hayashi) - *Paragondolella carpathica* (Mock) transitional form; upper view; 100x; sample GZ22bis (same level as GZ22); age: Carnian.
Fig. 19 - *Paragondolella noah* (Hayashi) - *Paragondolella carpathica* (Mock) transitional form; upper view; 100x; sample GZ22/23; age: Carnian.

PLATE 2

Fig. 1 - *Paragondolella noah* (Hayashi); upper-lateral view; 90x; sample GZ18; age: Carnian.
Fig. 2 - *Paragondolella noah* (Hayashi); upper-lateral view; 100x; sample GZ20; age: Carnian.
Fig. 3 - *Paragondolella carpathica* (Mock); lateral-upper view; 100x; sample GZ23; age: Carnian.
Fig. 4 - *Paragondolella noah* (Hayashi); lateral view; 100x; sample GZ20; age: Carnian.
Fig. 5 - *Paragondolella polygnathiformis* (Budurov & Stefanov) - *Paragondolella noah* (Hayashi) transitional form; lateral view; 100x; sample GZ18; age: Carnian.
Fig. 6 - *Paragondolella carpathica* (Mock); upper view; 90x; sample GZ23; age: Carnian.
Fig. 7 - *Paragondolella polygnathiformis* (Budurov & Stefanov) - *Paragondolella noah* (Hayashi) transitional form; upper-lateral view; 100x; sample GZ18; age: Carnian.
Fig. 8 - *Paragondolella noah* (Hayashi); upper view; 100x; sample GZ23; age: Carnian.
Fig. 9 - *Paragondolella carpathica* (Mock); upper view; 100x; sample GZ23; age: Carnian.
Fig. 10 - *Paragondolella carpathica* (Mock); lower view; 100x; sample GZ23; age: Carnian.
Fig. 11 - *Metapolygnathus nodosus* (Hayashi); lower-lateral view; 100x; sample GZ24; age: late Carnian-early Norian.
Fig. 12 - *Metapolygnathus nodosus* (Hayashi); upper view; 100x; sample GZ24; age: late Carnian-early Norian.
Fig. 13-14- *Metapolygnathus nodosus* (Hayashi); over view and upper-lateral view, respectively; 100x; sample GZ24; age: late Carnian-early Norian.
Fig. 15 - *Paragondolella noah* (Hayashi) – *Paragondolella carpathica* (Mock); lateral view, 100x, sample GZ 23; age Carnian.
Fig. 16 - *Paragondolella noah* (Hayashi) - *Paragondolella carpathica* (Mock); over-lateral view, 100x, sample GZ 23; age Carnian.
Fig. 17 - *Paragondolella carpathica* (Mock); upper-lateral view; 100x; sample GZ25; age: early Norian.

PLATE 3

Fig. 1 - *Epigondolella primitia* (Mosher); upper view; 100x; sample GZ25; age: early Norian.
Fig. 2 - *Epigondolella primitia* (Mosher); upper view; 90x; sample GZ25; age: early Norian.
Fig. 3 - *Epigondolella abneptis* (Huckriede); lateral-upper view; 100x; sample GZ26; age: early Norian.
Fig. 4 - *Epigondolella primitia* (Mosher); lateral-upper view; 90x; sample GZ25; age: early Norian.
Fig. 5 - *Epigondolella abneptis* (Huckriede) - *Ep. spatulata* (Hayashi); lateral-over view; 100x; sample GZ32; age early Norian.
Fig. 6 - *Epigondolella abneptis* (Huckriede); lateral view; 100x; sample GZ27; age: early Norian.
Fig. 7 - *Epigondolella abneptis* (Huckriede) - *Epigondolella spatulata* (Hayashi) transitional form; upper-lateral view; 100x; sample GZ29; age: early Norian.
Fig. 8 - *Epigondolella abneptis* (Huckriede); upper-lateral view; 100x; sample GZ27; age: early Norian.
Fig. 9 - *Epigondolella* aff. *abneptis* (Huckriede); lateral view;100x; sample GZ32; age: early Norian.
Fig. 10 - *Epigondolella quadrata* Orchard; over-lateral view; 100x; sample GZ32; age: early Norian.
Fig. 11 - *Epigondolella abneptis* (Huckriede) - *Epigondolella spatulata* (Hayashi) transitional form; lateral view; 100x; sample GZ30; age: early Norian.
Fig. 12 - *Epigondolella quadrata* Orchard; upper view; 100x; sample GZ29; age: early Norian.
Fig. 13 - *Epigondolella abneptis* (Huckriede) form transitional to *Epigondolella spatulata* (Hayashi); upper view; magnification 100x; sample GZ32; age: early Norian.
Fig. 14 - *Epigondolella abneptis* (Huckriede) - *E. spatulata* (Hayashi); upper view; 100x; sample GZ32; age: middle Norian.
Fig. 15 - *Epigondolella abneptis* (Huckriede) – *Epigondolella spatulata* (Hayashi) transitional form; upper view; 100x; sample GZ29; age: early Norian.

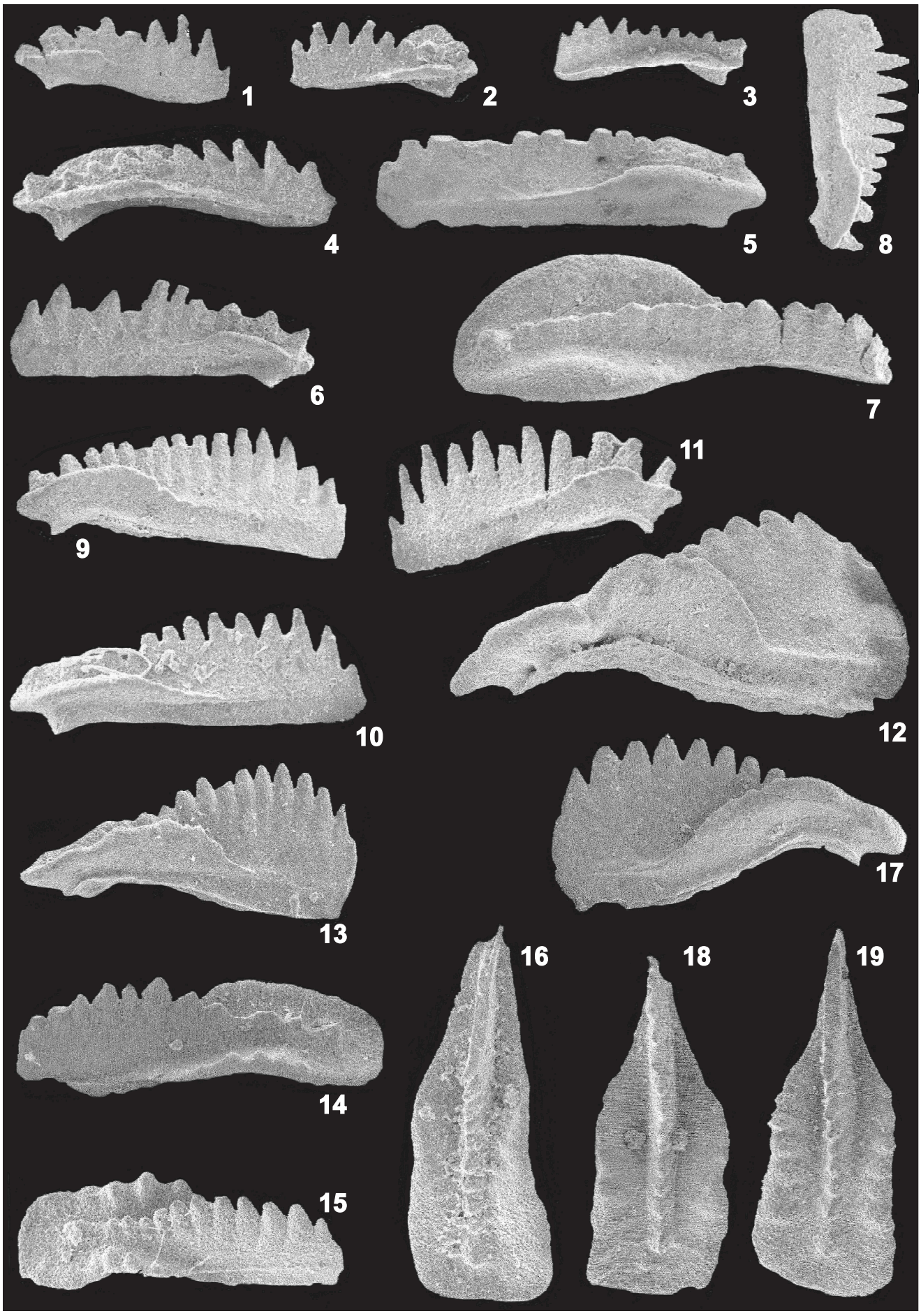


PLATE 1

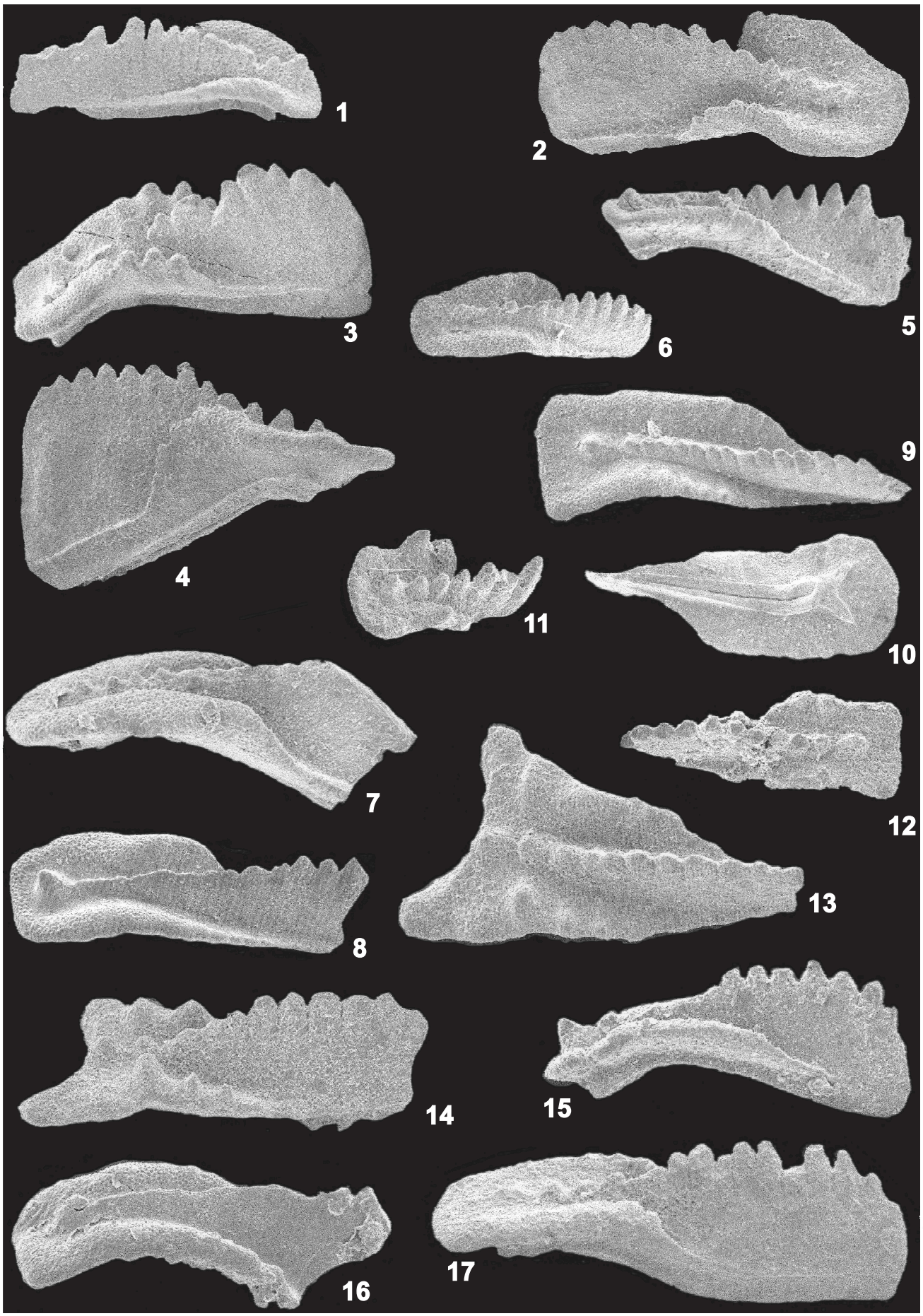


PLATE 2

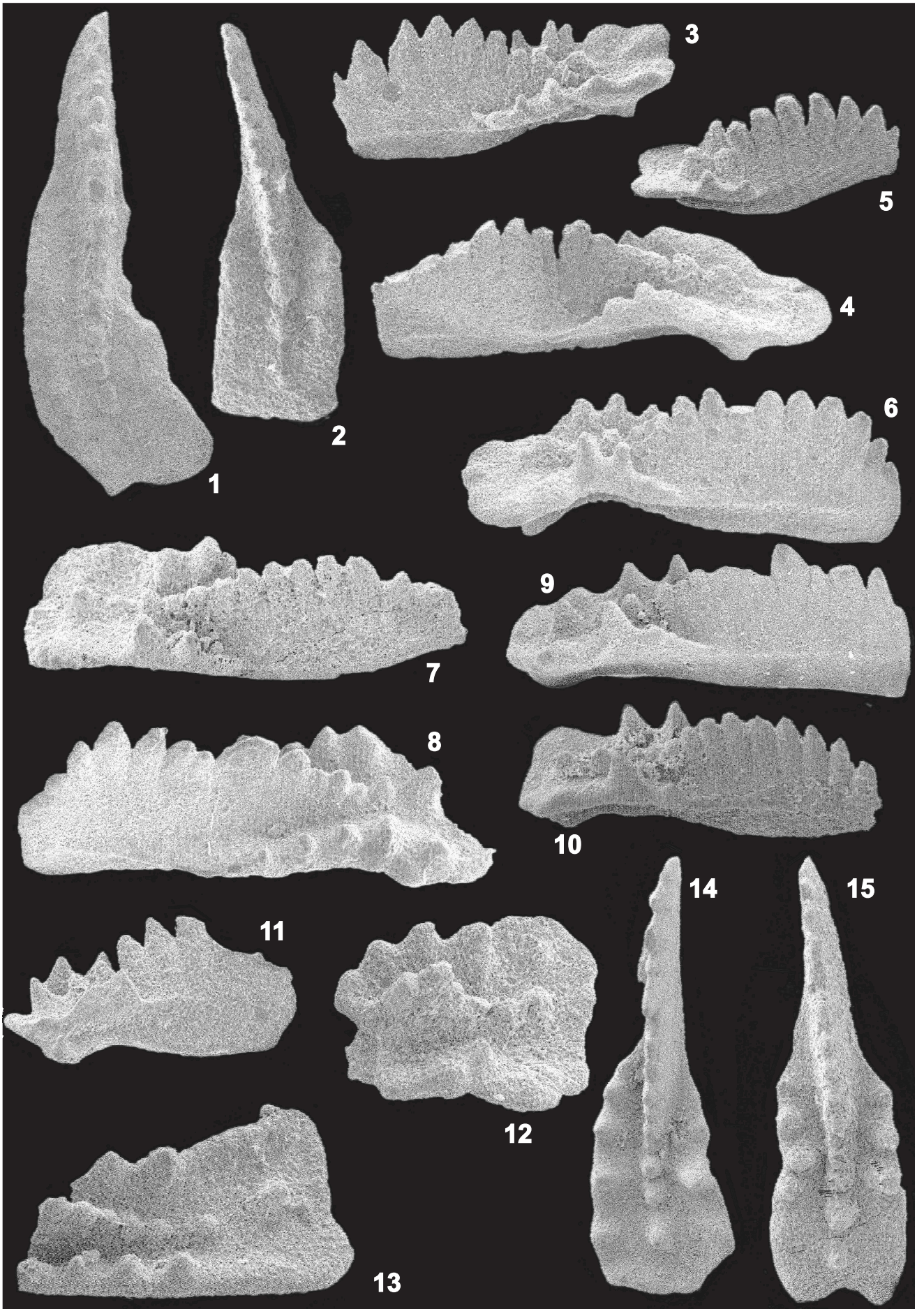


PLATE 3

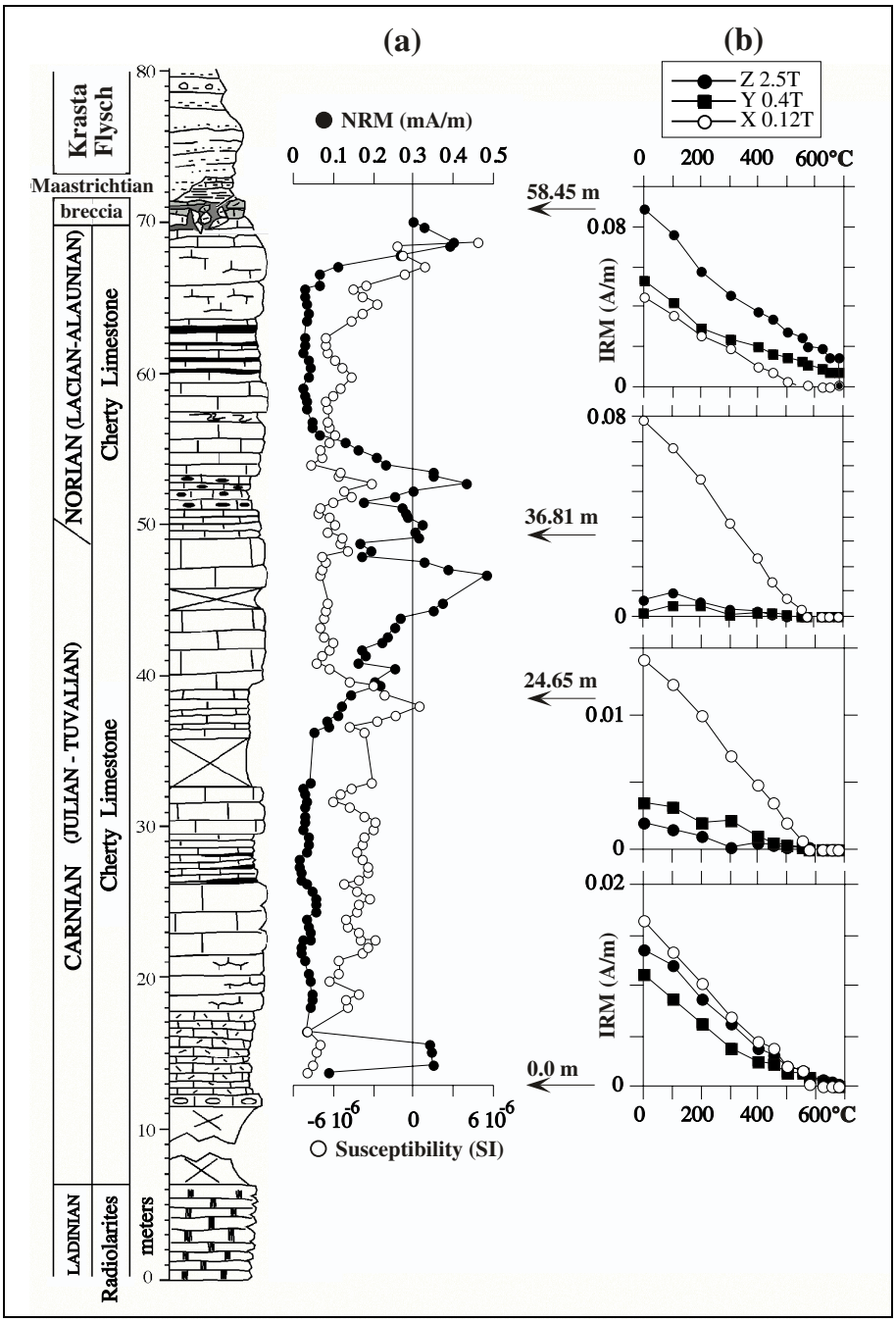


Fig. 3 - (a) The intensities of the natural remanent magnetization (NRM) and initial susceptibility at room temperature are plotted as a function of stratigraphic depth; (b) basic rock-magnetic properties have been studied by thermal decay of a 3-component isothermal remanent magnetization (IRM). See text for discussion.

| | In Situ | | | | | | | | | Tilt Corrected | | | | | | | | |
|---|---|---|---|---|---|---|---|---|---|---|---|---|---|---|---|---|---|---|
| | $N_1/N_2$ | Dec. (°E) | Inc. (°) | k | $\alpha_{95}$ (°) | Lat. (°N) | Long. (°E) | dp/dm (°) | Plat. (°N) | Dec. (°E) | Inc. (°) | k | $\alpha_{95}$ (°) | Lat. (°N) | Long. (°E) | dp/dm (°) | Plat. (°N) |
| GURI ZI PALEOMAGNETIC DIRECTIONS AND POLES: | | | | | | | | | | | | | | | | | | |
| "B" component[1] | 110/36 | 219.6 | -26.3 | 12 | 7.2 | 45.6 | 136.4 | 4.2/7.8 | 14 | 219.1 | 22.2 | 14 | 6.5 | | | | | |
| "Ch" component | 110/89 | 141.9 | 60.1 | 8 | 5.7 | | | | | 88.1 | 32.4 | 9 | 5.2 | 13.1 | 97.0 | 3.3/5.9 | 18 ± 4 | |
| LATE TRIASSIC-EARLY JURASSIC REFERENCE PALEOMAGNETIC DIRECTION AND POLE[2]: | | | | | | | | | | | | | | | | | | |
| | N = 4 | | | | | | | | | 354.5 | 41.3 | | | 71.1 | 214.8 | $A_{95}$= 4.3 | 24 ± 3 | |

$N_1$: number of standard 11 cc specimens collected. $N_2$: number of paleomagnetic directions used to calculate the mean. Dec., Inc.: declination and inclination, in geographic or tilt corrected coordinates. k, $\alpha_{95}$: Fisher precision parameter and radius of cone of 95% confidence about the mean direction, respectively.

Lat., Long.: paleomagnetic pole latitude and longitude. K, dp/dm: Fisher precision parameter and axes of the 95% ellipse of confidence about the mean pole, respectively. A95: radius of cone of 95% confidence about the mean pole. Plat.: paleolatitude expressed in °N.

[1] Stable endpoint directions only.

[2] From Muttoni et al. (2001b).

Tab. 1 - Paleomagnetic directions and paleomagnetic poles from Guri Zi (Lat.=42.05°N, Long. = 19.02°E).

**Rock-magnetic properties and paleomagnetic directions**

The mean intensity of the natural remanent magnetization (NRM) is 0.1 mA/m and increases up to 0.5 mA/m in the middle part of the section. The room temperature magnetic susceptibility is in the diamagnetic range (i.e., small negative values) and does not follow the NRM intensity trend (Fig. 3a).

Thermal unblocking characteristics of orthogonal components of isothermal remanent magnetization (IRM) (Lowrie 1990) revealed the presence of a dominant low coercivity and ~570 °C maximum unblocking temperature phase interpreted as magnetite, coexisting, in the uppermost part of the section, with a subsidiary high-coercivity and ~680 °C maximum unblocking temperature phase interpreted as hematite (Fig. 3b).

Stepwise thermal demagnetization was applied to isolate magnetic components of the NRM. Samples typically show the presence of a linear "A" component of magnetization isolated by means of least-square line-fits (Kirschvink 1980) on vector endpoint demagnetization diagrams between room temperature and ~200 °C. This component has *in situ* steep positive inclinations (Fig. 4) and is broadly consistent with viscous magnetization acquired along the present-day field direction (Fig. 5; Dec = 18 °E, Inc = 65°). In the temperature range between ~200 °C and 300-350 °C, a linear "B" component overprint with *in situ* southwest and negative directions was resolved in 33% of the samples. In the remaining 66% of the samples, this "B" component of magnetization migrates along great circle paths toward a dual polarity characteristic ("Ch") component with either southeast and positive or northwest and negative *in situ* directions (Figs. 4, 5). "Ch" endpoint components were successfully isolated in 81% of the samples between ~400 °C and ~550 °C up to a maximum of 680 °C (Figs.

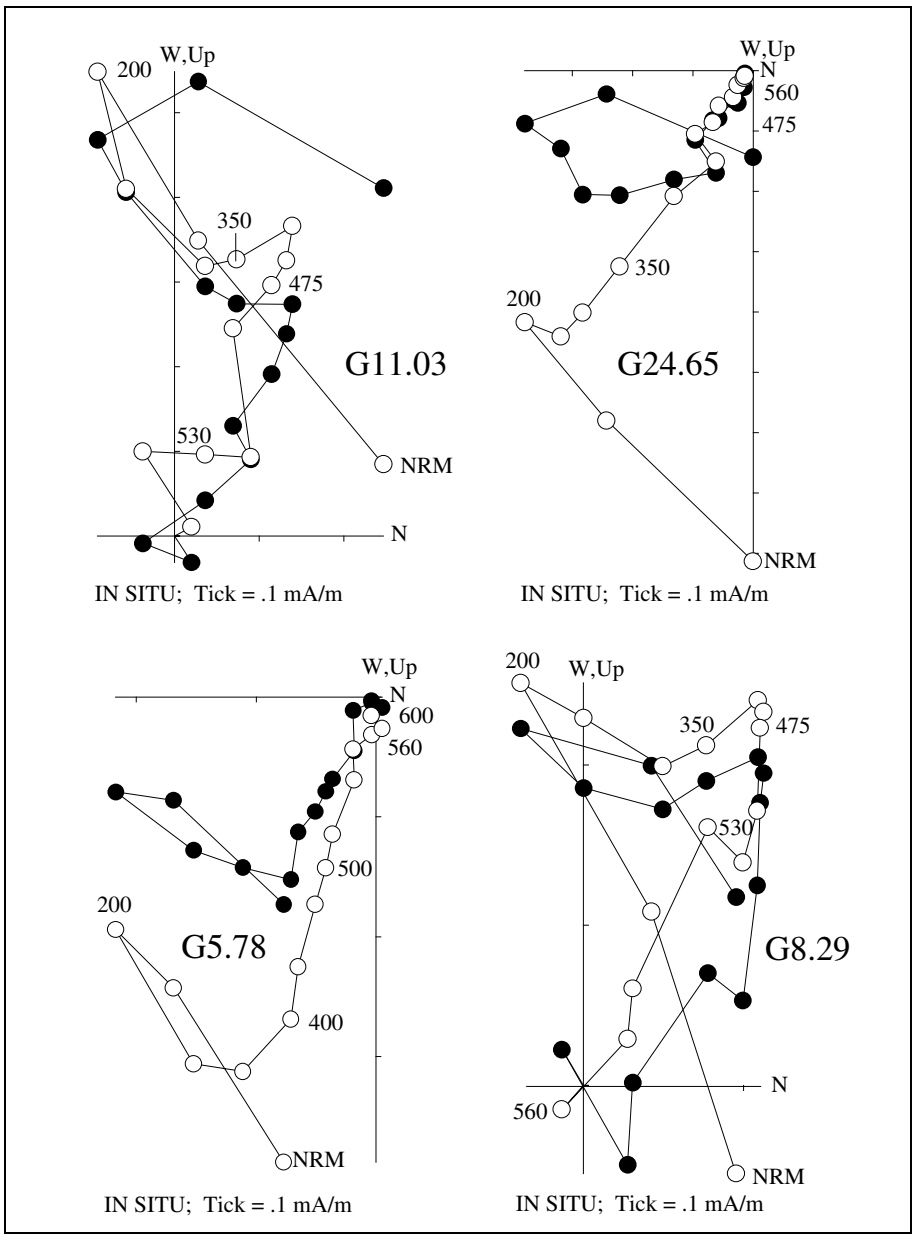


Fig. 4 - Zijderveld thermal demagnetization diagrams of the NRM of representative samples from Guri Zi bearing normal (G24.65, G5.78) and reverse (G11.03, G8.29) polarity magnetization. Closed (open) symbols are projections onto the horizontal (vertical) plane in *in situ* coordinates. Demagnetization temperatures expressed in °C.

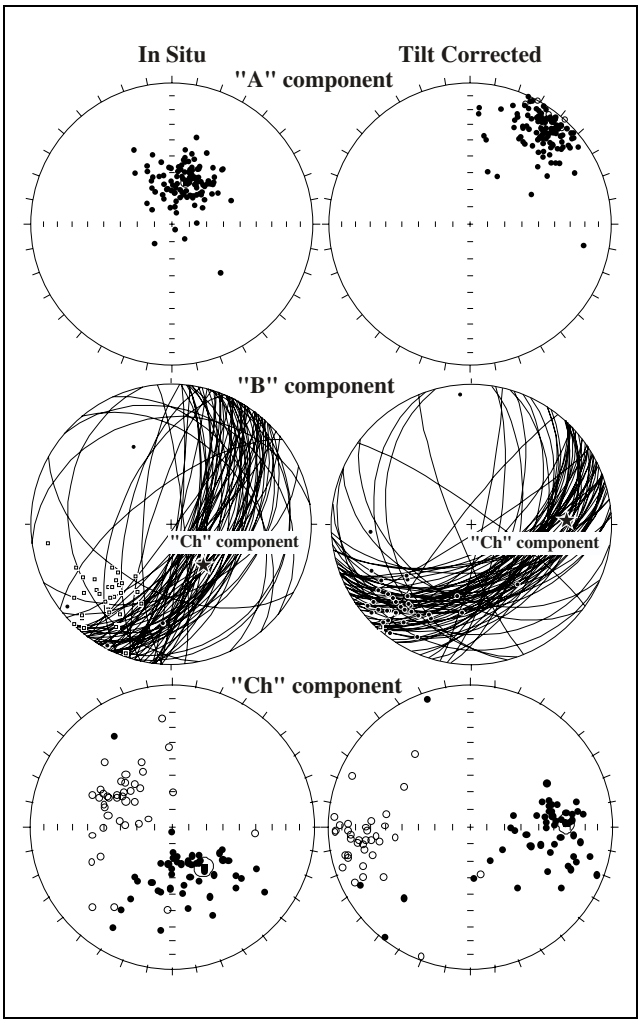


Fig. 5 - Equal-area projections before (*in situ*) and after bedding tilt correction of the "A", "B", and "Ch" endpoint component directions, and of the "B" component remagnetization great circles. See text for discussion.

4, 5). The "Ch" components turn east and positive or west and negative after application of bedding tilt correction (Fig. 5; Tab. 1). Although normal and reverse populations are clearly seen, their means depart from antipodality by ~23° and the reversal test *sensu* McFadden & McElhinny (1990) resulted negative. We attribute this departure from antipodality to residual contamination of the "Ch" by the "B" component overprint. In order to minimize this biasing effect, we invert the reverse "Ch" directions to common normal polarity and calculate an overall mean direction of Dec = 88.1 °E, Inc = 32.4° ($a_{95}$ = 5.2°, k = 9, N = 89).

## Magnetostratigraphy

We interpret the "Ch" component in tilt corrected coordinates as the original Triassic magnetization. The stratigraphic evolution of Albania has Gondwanan affinity, therefore, we assume that the "Ch" and "B" components were originated at or close to the northern margin of Africa, which was located in the northern hemisphere during the Meso-Cenozoic (e.g., Muttoni et al. 1996a; Dercourt et al. 2000; Stampfli 2000). Consequently, positive "Ch" directions represent normal polarity, whereas negative ones represent reverse polarity. A virtual geomagnetic pole (VGP) was calculated for each "Ch" component direction in tilt corrected coordinates. The latitude of the specimen VGP with respect to the overall mean north paleomagnetic pole was used to delineate magnetic polarity stratigraphy. VGP relative latitudes approaching +90°N or -90°N were interpreted as recording normal or reverse polarity, respectively. For polarity magnetozone identification, we adopted the nomenclature used by Kent et al. (1995). The latitude of the specimens VGPs defines

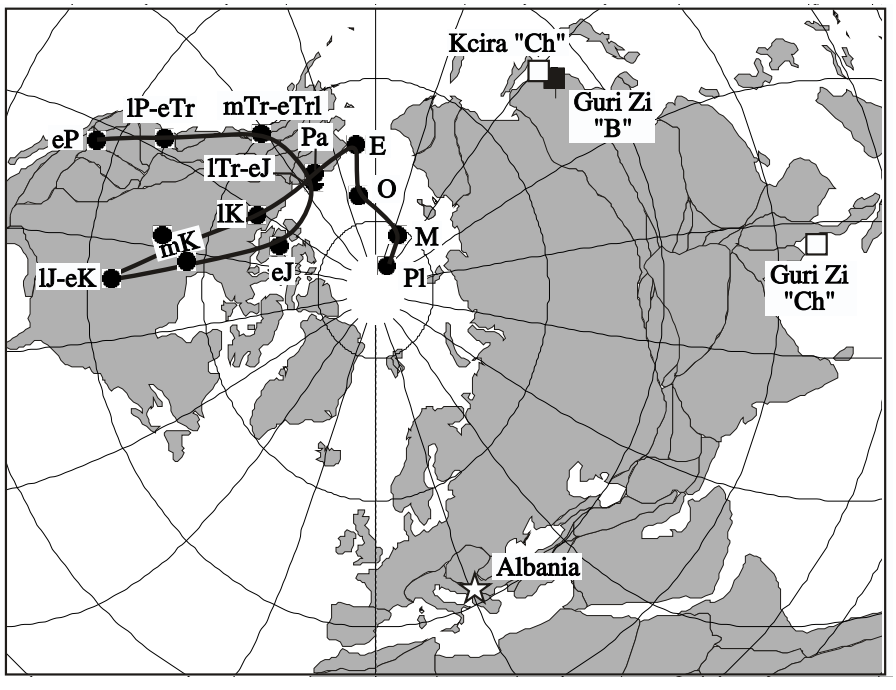


Fig. 6 - The paleomagnetic poles from Guri Zi and Kçira (squares) are compared to the Gondwanan apparent polar wander path (solid circles). The suffix attached to the pole designation refers to the magnetization component used to calculate the pole: "Ch" is the characteristic component, "B" a secondary component. eP is Early Permian, lP is Late Permian, eTr is Early Triassic, mTr is Middle Triassic, eTrl is early Late Triassic, lTr is Late Triassic, eJ is Early Jurassic, lJ is late Jurassic, eK is Early Cretaceous, mK is Mid Cretaceous, lK is Late Cretaceous, Pa is Paleocene, E is Eocene, O is Oligocene, M is Miocene, Pl is Pliocene. See text for discussion.

at Guri Zi a sequence of 14 magnetozones from GZ1r to GZ8n (Fig. 2).

**Paleomagnetic poles**

The Late Triassic "Ch" component at Guri Zi in the Krasta-Cukali Zone gives a paleomagnetic pole (paleopole) rotated ~85° clockwise with respect to the Late Triassic-Early Jurassic reference paleopole of Gondwana (Muttoni et al. 2001b) (Fig. 6; Tab. 1). A "Ch" component of Middle Triassic age was observed at Kçira in the External Mirdita Zone (Muttoni et al. 1996b) (Fig. 1). It defines a paleopole rotated ~40°-45° clockwise with respect to the reference paleopole of Gondwana of corresponding age (Fig. 6). The age of acquisition of the "B" component at Guri Zi is unknown; it is here conservatively considered post-folding because its paleopole plotted in *in situ* coordinates is by far less removed from the Gondwanan apparent polar wander path then after bedding tilt correction. In detail, the "B" component paleopole is rotated ~40° clockwise with respect to the Late Cretaceous-Early Cenozoic Gondwana paleopoles, and falls close to the Kçira "Ch" component paleopole (Fig. 6).

Based on the above, we propose that Guri Zi in the Krasta-Cukali Zone rotated ~45° clockwise with respect to Gondwana after the acquisition of the "Ch" component in the Late Triassic and prior to the acquisition of the "B" component in the Late Cretaceous-Early Cenozoic. An additional ~40° clockwise rotation occurred after the acquisition of the "B" component in the Cenozoic in concert with rotations of External Mirdita Zone units as observed at Kçira (Fig. 6). Tectonic rotations of thrust sheets may be related to Alpine deformation, which in the Albanian belt commenced as early as latest Jurassic and continued into the Cenozoic. For example, the inferred post-"B" component clockwise rotation at Guri Zi and Kçira may be associated with the rotation of the external zone of Albania since the Early-Middle Miocene (Speranza et al. 1995; Mauritsch et al. 1995).

**Correlation to literature sections and the age of the Carnian-Norian boundary**

Magnetostratigraphic and biostratigraphic data from Guri Zi are tentatively correlated to data from the Silicka Brezova marine limestone section from Slovakia (Channell et al. 2003), the Pizzo Mondello marine limestone section from Sicily (Muttoni et al. 2004), as well as the continental Newark astrochronological polarity time scale (APTS; Kent & Olsen 1999) (Fig. 7). Details on the correlation between Silicka Brezova, Pizzo Mondello, and the Newark APTS are given in Muttoni et al. (2004).

Guri Zi, Silicka Brezova, and Pizzo Mondello bear at a gross scale a similar assemblage of Carnian-Norian boundary conodonts comprising, among the most significant events:

(i) the LO of *Paragondolella polygnathiformis* (Guri Zi and Silicka Brezova) and the LO of the equivalent *Metapolygnathus polygnathiformis* (Pizzo Mondello);

(ii) the LO of *Metapolygnathus nodosus* (Guri Zi and Pizzo Mondello) and the LO of the equivalent *Epigondolella nodosa* (Silicka Brezova);

(iii) the FO of *Epigondolella primitia* (Guri Zi and Silicka Brezova);

(iv) the FO of *Neogondolella navicula* (Silicka Brezova);

(v) the FO of *Metapolygnathus communisti* (Pizzo Mondello);

(vi) the FO of *Epigondolella abneptis* (Guri Zi and Silicka Brezova).

These biostratigraphic events define at Silicka Brezova and Pizzo Mondello a Carnian-Norian boundary that was magnetostratigraphically traced onto Newark magnetozone E7 in the ~228-227 Ma interval (Fig. 7; Muttoni et al. 2004). Guri Zi magnetozones GZ3n to GZ7r may correlate to magnetozones SB-3n to SB-3r at Silicka Brezova and PM3n to PM4r at Pizzo Mondello, which correspond as a whole to magnetozone E7 in the Newark basin (Fig. 7). In particular, Guri Zi magnetozone GZ6n containing the Carnian-Norian boundary may correlate to SB-3n at Silicka Brezova, PM3n at Pizzo Mondello, and E7n in the Newark basin. This being the case, the location of the Carnian-Norian boundary onto the Newark APTS would find additional confirmation. The correlation between Guri Zi and Pizzo Mondello-Silicka Brezova-Newark APTS is at places visually elusive because of distortion of the magnetostratigraphic sequence by variations in sedimentation rate triggered by turbiditic redeposition of calcarenites.

**Conclusions**

The following conclusions can be drawn from this analysis. Biostratigraphic data from Guri Zi indicate the occurrence of the Carnian-Norian boundary at around meter level 50 between the last occurrence of *Metapolygnathus nodosus* and the first occurrence of *Epigondolella abneptis.* This boundary has been magnetostratigraphically traced onto Newark magnetozone E7 dated at ~228-227 Ma (adopting Newark astrochronology). Finally, paleomagnetic pole position analysis indicates that a complex history of clockwise tectonic rotations - still poorly resolved - occurred in the Balkan region since Triassic times.

*Repository.* The conodont identification are made by S. Meço and conodont specimens are stored in Palaeontological Cabinet at the Faculty of Geology and Minino (FGJM) Rr. Labinoti, Tirana, Albania in the box XI under the label KrZ (Krasta Zone) GZ (Guri Zi) and the figure of the level.

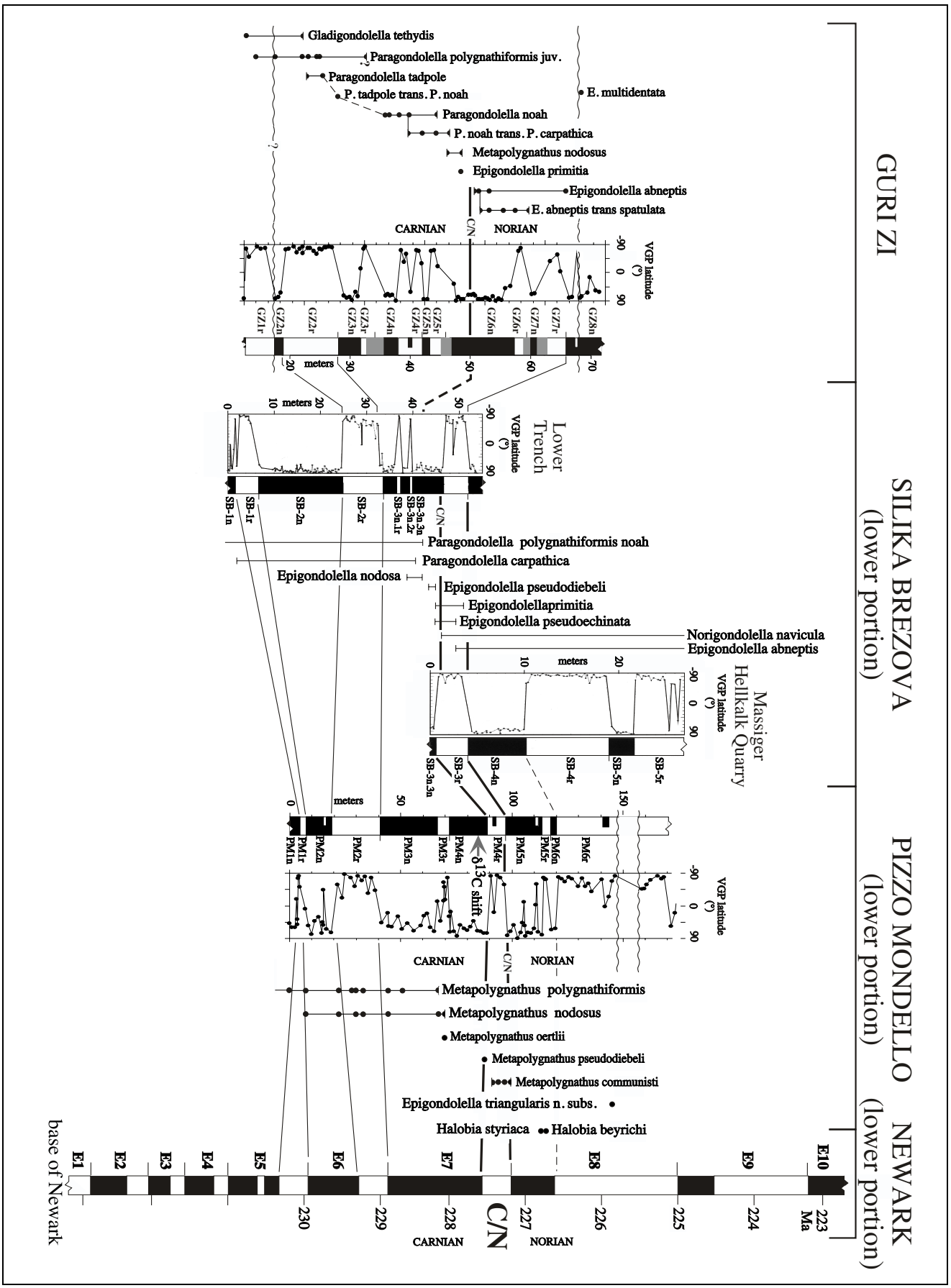


Fig. 7 - Comparison of magnetostratigraphic and biostratigraphic data from this study and the literature across the Carnian-Norian boundary. The Guri Zi section is tentatively correlated to the lower part of the Silicka Brezova section of Channell et al. (2003), the lower part of the Pizzo Mondello section of Muttoni et al. (2004), as well as the lower part of the Newark APTS (Kent & Olsen 1999). See text for discussion.

*Acknowledgements*. Spartak Fejzollari, Tirana, helped in the field and prepared the conodont samples. H. Mostler, Innsbruck, discussed the conodont identification; A. Nicora, Milano, M. Orchard, Vancouver, and Roberto Lanza, Torino, reviewed an earlier version of the paper. Financial support partially provided by the Italian-Albanian agreement of scientific cooperation.

## REFERENCES

Channell J. E. T., Kozur H. W., Sievers T., Mock R., Aubrecht R. & Sykora M. (2003) - Carnian-Norian biomagnetostratigraphy at Silicka Brezova (Slovakia): correlation to other Tethyan sections and to the Newark Basin. *Paleogeogr., Palaeoclimatol., Palaeoecol.,* 191: 65-109, Amsterdam.

Dercourt J., Gaetani M., Vrielynck B., Barrier E., Biju-Duval B., Brunet M.F., Cadet J.P., Crasquin S., Sandulescu M. (2000) - Atlas Peri-Tethys. Palaeogeogeographic maps. 24 maps and explanatory notes: I-XX, 1-269. CCGM/CGMW, Paris.

Gallet Y., Besse J., Krystyn L., Marcoux J., Guex J. & Theveniaut H. (2000) - Magnetostratigraphy of the Kavaalani section (southwestern Turkey): Consequence for the origin of the Antalya Calcareous Nappes (Turkey) and for the Norian (Late Triassic) magnetic polarity timescale. *Geophys. Res. Lett*., 27: 2033-2036, Washington, DC.

Godroli M. (1992) - Tectonique des ophiolites dans les Albanides internes: modalites d'ouverture et de fermeture d'un bassin oceanique etroit (exemple des ophiolites de la zone de Mirdita). Ph.D. thesis, Université de Paris-Sud, centre d'Orsay, Paris.

Kellici I., De Wever P. & Kodra A. (1994) - Mesozoic radiolarians from different sections of the Mirdita nappe, Albania. Paleontology and stratigraphy. *Rev. Micropaleont*., 37: 209-222, Paris.

Kent D. V. & Olsen P. E. (1999) - Astronomically tuned geomagnetic polarity time scale for the Late Triassic. *J. Geophys. Res.*, 104: 12,831-12,841, Washington, DC.

Kent D. V., Olsen P. E. & Witte W. K. (1995) - Late Triassic-earliest Jurassic geomagnetic polarity reference sequence from cyclic continental sediments of the Newark Rift Basin (eastern North America). *Albertiana*, 16: 17-26, Utrecht.

Kirschvink J. L. (1980) - The least-squares line and plane and the analysis of palaeomagnetic data. *Geophys. J. Royal Astron. Soc*., 62: 699-718, Oxford, Edinburgh.

Krystyn L., Gallet Y., Besse J. & Marcoux J. (2002) - Integrated Upper Carnian to Lower Norian biochronology and implications for the Upper Triassic magnetic polarity time scale. *Earth Planet. Sci. Lett*., 203: 343-351, Amsterdam.

Lowrie W. (1990) - Identification of ferromagnetic minerals in a rock by coercivity and unblocking temperature properties. *Geophys. Res. Lett*., 17: 159-162, Washington, DC.

Mauritsch H. J., Scholger R., Bushati S. L. & Ramiz H. (1995) - Palaeomagnetic results from southern Albania and their significance for the geodynamic evolution of the Dinarides, Albanides and Hellenides. *Tectonophysics,* 242: 5-18, Amsterdam.

McFadden P. L. & McElhinny M. W. (1990) - Classification of the reversal test in palaeomagnetism. *Geophys. J. Int*., 103: 725-729, Oxford, Edinburgh.

Meço S. (1999) - Conodont biostratigraphy of Triassic pelagic strata, Albania. *Riv. It. Paleont. Strat.*, 105: 251-266, Milano.

Meço S. & Aliaj S. (2000) - Geology of Albania, v. of 246 pp., Gebr. Borntraeger, Berlin.

Muttoni G., Kent D. V. & Channell J. E. T. (1996a) - Evolution of Pangea: Paleomagnetic constraints from the Southern Alps, Italy. *Earth Planet. Sci. Lett*., 140: 97-112, Amsterdam.

Muttoni G., Kent D. V., Meço S., Nicora A., Gaetani M., Balini M., Germani D. & Rettori R. (1996b) - Magnetobiostratigraphy of the Spathian to Anisian (Lower to Middle Triassic) Kçira section, Albania. *Geophys. J. Int*., 127: 503-514, Oxford.

Muttoni G., Kent D. V., Di Stefano P., Gullo M., Nicora A., Tait J. & Lowrie W. (2001a) - Magnetostratigraphy and biostratigraphy of the Carnian/Norian boundary interval from the Pizzo Mondello section (Sicani Mountains, Sicily). *Paleogeogr., Palaeoclimatol., Palaeoecol.,* 166: 383-399, Amsterdam.

Muttoni G., Garzanti E., Alfonsi L., Cirilli S., Germani D. & Lowrie W. (2001b) - Motion of Africa and Adria since the Permian: paleomagnetic and paleoclimatic constraints from northern Libya. *Earth Planet. Sci. Lett*., 192: 159-174, Amsterdam.

Muttoni G., Kent D. V., Olsen P. E., Di Stefano P., Lowrie W., Bernasconi S. & Martín Hernández F. (2004) - Tethyan magnetostratigrapy from Pizzo Mondello and correlation to the Late Triassic Newark APTS. *Geol. Soc. Am. Bull.*, 116(9/10): 1043-1058, Boulder.

Robertson A. H. F., Clift P. D., Degnan P. J. & Jones G. (1991) - Palaeogeographic and palaeotectonic evolution of the Eastern Mediterranean Neotethys. *Paleogeogr., Palaeoclimatol., Palaeoecol.,* 87: 289-343, Amsterdam.

Shallo M. (1992) - Geological Evolution of the Albanian Ophiolites and their platform periphery. *Geol. Rundsch*., 81: 681-694, Berlin.

Shallo M. (1994) - Outline of the Albanian ophiolites. *Ofioliti*, 19/1: 57-75, Pisa.

Speranza F., Islami I., Kissel C. & Hyseni A. (1995) - Paleomagnetic evidence for Cenozoic clockwise rotation of the external Albanides. *Earth Planet. Sci. Lett*., 129: 121-134, Amsterdam.

Stampfli G.M. (2000) - Tethyan Oceans. In: Bozkurt E., Winchester J.A. & Piper J.D.A. (eds.) - Tectonics and Magmatism in Turkey and the Surrounding Area. *Geol. Soc. London, Spec. Publ.,* 173: 1-23, London.